

Beyond maps: Patterns of formation processes at the Middle Pleistocene open-air site of Marathousa 1, Megalopolis Basin, Greece

D. Giusti^{a,*}, V. Tourloukis^a, G. E. Konidaris^a, N. Thompson^b, P. Karkanas^c,
E. Panagopoulou^d, K. Harvati^a

^a*Paläoanthropologie, Senckenberg Centre for Human Evolution and Palaeoenvironment, Eberhard Karls Universität Tübingen, Rümelinstr. 23, 72070 Tübingen, Germany*

^b*Friedrich-Alexander University of Erlangen-Nürnberg, Institute of Prehistory and Early History, Kochstr. 4/18, 90154 Erlangen, Germany*

^c*Malcolm H. Wiener Laboratory for Archaeological Science, American School of Classical Studies at Athens, Greece*

^d*Ephoreia of Palaeoanthropology-Speleology of Greece, Athens, Greece*

Abstract

Recent excavations at the Middle Pleistocene open-air site of Marathousa 1 have unearthed in one of the two investigated area (Area A) a partial skeleton of a single individual of *Elephas (Palaeoloxodon) antiquus* and other faunal remains in spatial and stratigraphic association with lithic artefacts. In Area B, a much higher number of lithic artefacts was collected, spatially and stratigraphically associated with other faunal remains. The two areas are stratigraphically correlated, the main fossiliferous layers representing an *en masse* depositional process in a lake margin context. Evidence of butchering (cut-marks) has been identified on two bones of the elephant skeleton, as well on other mammal bones from Area B. However, due to the secondary deposition nature of the main find-bearing units, it is of primary importance to evaluate the degree and reliability of the spatial association of the lithic artefacts with the faunal remains. Indeed, spatial association does not necessarily imply causation. The present study uses a comprehensive set of multiscale and multivariate spatial statistics, in order to disentangle the depositional processes behind the distribution of the archaeological and palaeontological record at Marathousa 1. Moving beyond distribution maps,

*Corresponding author

Email address: domenico.giusti@uni-tuebingen.de (D. Giusti)

statistical inference allows for a better interpretation of spatial patterns by adopting a more inductive and reproducible strategy. Moreover, within a frame of references, it enables us to depict the underlying processes responsible for the observed patterns, and to quantify the extent of the post-depositional reworking processes which have long been recognised to affect the integrity of archaeological assemblages. Assessing the degree of disturbance is crucial to fully comprehend the archaeological record, and therefore to reliably interpret past human behaviours. Preliminary results of our analyses suggest minor reworking and substantial spatial association of the lithic and faunal assemblages, supporting the current interpretation of Marathousa 1 as a butchering site.

Keywords: Spatial taphonomy, Vertical distribution, Fabric analysis, Point pattern analysis, Site formation processes, Middle Pleistocene

1. Introduction

The analysis of archaeological site formation and modification processes, intensively studied since the early 1970s ([Isaac, 1967](#); [Schiffer, 1972, 1983, 1987](#); [Shackley, 1978](#); [Wood and Johnson, 1978](#); [Schick, 1984, 1986, 1987](#); [Petruglia and Nash, 1987](#); [Petruglia and Potts, 1994](#), among others), is nowadays fully integrated in the archaeological practice. Drawing inferences about past human behaviours from scatters of archaeological remains must account for depositional and post-depositional contextual processes.

Several methods are currently applied in order to qualify and quantify the type and degree of reworking of archaeological assemblages. Within the framework of a geoarchaeological and taphonomic approach, spatial statistics offer meaningful contributions in unravelling site formation and modification processes from spatial patterns.

The study of the clast fabric (dip and strike of elongated sedimentary particles, including bones and artefacts), first addressed by [Isaac \(1967\)](#); [Bar-Yosef and Tchernov \(1972\)](#); [Schick \(1986\)](#), has more recently been found to successfully discriminate between sedimentary processes ([Bertran and Texier, 1995](#); [Bertran et al., 1997](#)), leading to a noteworthy development of methods and propagation of applications in Palaeolithic site formation studies ([Lenoble and Bertran, 2004](#); [Lenoble et al., 2008](#); [McPherron,](#)

2005; Benito-Calvo et al., 2009; Benito-Calvo and de la Torre, 2011; Benito-Calvo et al., 2011; Bernatchez, 2010; Domínguez-Rodrigo et al., 2012; García-Moreno et al., 2016; Sánchez-Romero et al., 2016, among others).

The vertical distribution of materials, on the other hand, has been long investigated with the aim of identifying cultural levels, by visually interpreting virtual profiles (but see Anderson and Burke (2008) for a quantitative approach).

However, archaeological horizons may be subject to vertical rearrangement by syn- and post-depositional processes. Several experimental studies have investigated the effect of trampling on the vertical displacement of artefacts (Villa and Courtin, 1983; Gifford-Gonzalez et al., 1985; Nielsen, 1991; Eren et al., 2010). Although these works have reported a negative correlation between artefact size and vertical displacement, particle size sorting of lithic assemblages, when exposed to physical geomorphic agents (such as gravity, water flow, waves and tides, wind), has been widely documented (Rick, 1976; Schick, 1986; Petraglia and Nash, 1987; Morton, 2004; Lenoble, 2005; Bertran et al., 2012).

Bone and lithic refitting analysis is an additional, particularly robust method in investigating the stratigraphic integrity of a site (Villa, 1982, 1990; Todd and Stanford, 1992; Morin et al., 2005; Sisk and Shea, 2008). Furthermore, lithic refits have been shown to provide reliable clues about the spatio-temporal dimension of past human behaviours, by discriminating activity areas (López-Ortega et al., 2011, 2015; Vaquero et al., 2012, 2015; Clark, 2016).

Finally, distribution maps are cornerstones of the archaeological documentation process and are primary analytic tools. However, their visual interpretation is prone to subjectivity and is not reproducible. Since the early 1970's (see Hodder and Orton (1976); Orton (1982) and references therein), the traditional, intuitive, 'eyeballing' method of spotting spatial patterns has been abandoned in favour of more objective approaches, extensively borrowed from other fields. Nevertheless, quantitative methods, while still percolating in the archaeological sciences from neighbouring disciplines, are not extensively used. Moreover, only a relatively small number of studies have explicitly applied spatial point pattern analysis or geostatistics to the study of site formation and modification processes (Lenoble et al., 2008; Domínguez-Rodrigo et al., 2014b,a,

2017; Carrer, 2015; Giusti and Arzarello, 2016; Organista et al., 2017, but see Hivernel and Hodder (1984) for an earlier work on the subject).

The goal of a taphonomic approach to spatial analysis is to move beyond distribution maps by applying a comprehensive set of multiscale and multivariate spatial statistics, in order to reliably infer processes from spatial patterns. An exhaustive spatial analytic approach to archaeological inference, combined with a taphonomic perspective, is essential for the evaluation of the integrity of the archaeological assemblage, and consequently for a reliable interpretation of past human behaviours.

2. Marathousa 1

The object of the present study is the spatial distribution of the archaeological and palaeontological record recovered during excavation at the Middle Pleistocene open-air site of Marathousa 1, Megalopolis, Greece (Panagopoulou et al., 2015; Harvati et al., 2016).

The site (Fig. 1), discovered in 2013 at the edge of an active lignite quarry, is located between lignite seams II and III in the Pleistocene deposit of the Megalopolis basin, Marathousa Member of the Choremi Formation (van Vugt et al., 2000). The regular alternation of lacustrine clay, silt and sand beds with lignite seams has been interpreted having cyclic glacial (or stadial) and interglacial (or interstadial) origin (Nickel et al., 1996). The half-graben configuration of the basin, with major subsidence along the NE-SW trending normal faults at the eastern margin, resulted in the gentle dip of the lake bottom at the opposite, western, margin of the lake, enabling the formation of swamps and the accumulation of organic material for prolonged periods of time (van Vugt et al., 2000).

Two excavation areas have been investigated since 2013: Area A, where several skeletal elements of a single individual of *Elephas (Palaeoloxodon) antiquus* have been unearthed, together with a number of lithic artefacts (Konidaris et al., this volume; Tourloukis et al., this volume); and Area B, about 60 m to the South along the exposed section, where the lithic assemblage is richer and occurs in association with a faunal assemblage composed by isolated elephant bones, cervids and carnivores among others.

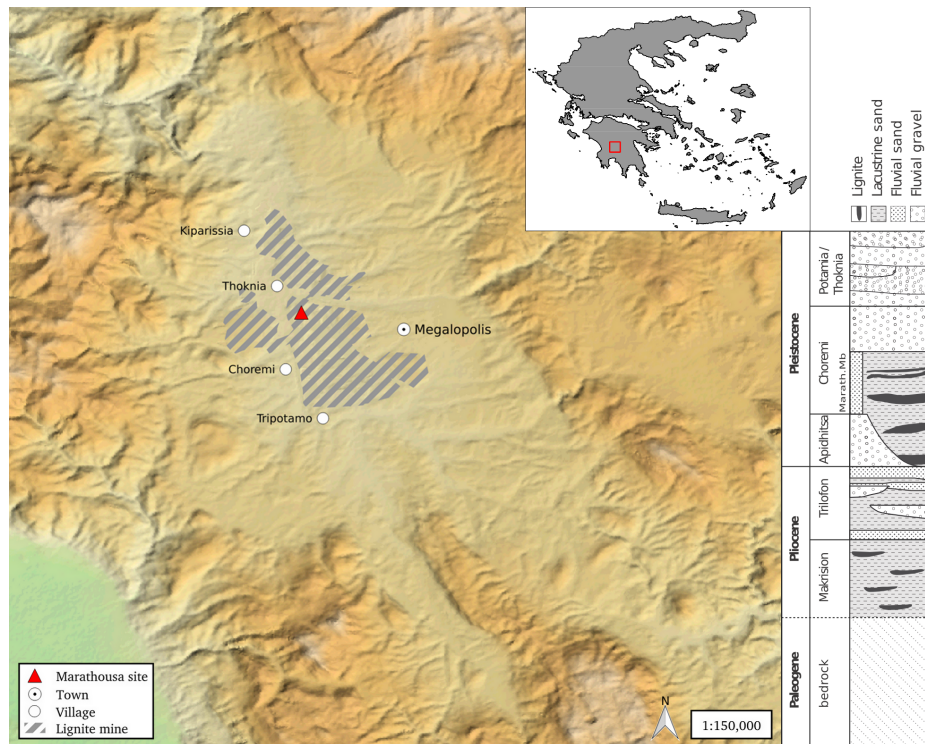


Figure 1: Geographical location of the Marathousa 1 site in the Megalopolis basin and stratigraphic column, modified after [van Vugt et al. \(2000\)](#).

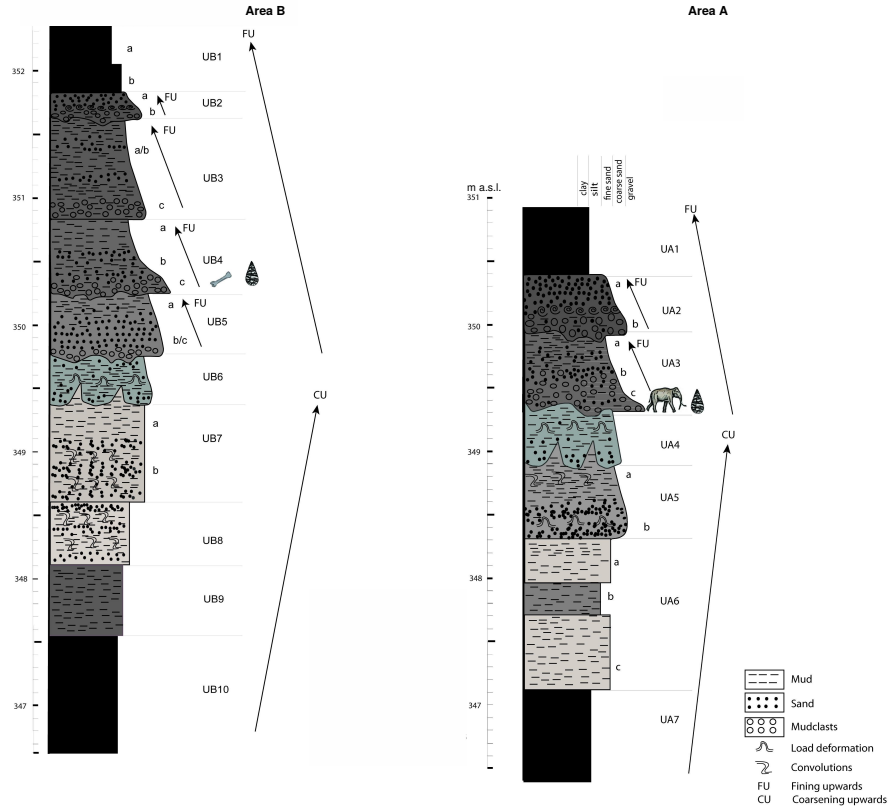


Figure 2: Stratigraphic setting of the Marathousa 1 site, modified after Karkanas et al. (this volume).

Evidence of butchering (cut-marks) have been identified on two of the elephant bones from Area A, as well on elephant and other mammal bones from Area B (Konidaris et al., this volume).

An erosional contact separates the two main find-bearing units in both areas, namely UA3c/4 and UB4c/5a (Fig. 2). In Area A, the elephant remains lie at the contact of UA3c/4 and are covered by UA3c. In Area B, most of the material were collected from unit UB4c. For both areas, the working hypothesis is that the flow event represented by units UA3c and UB4c eroded an exposed surface (where the elephant was lying) and scoured this surface, thereby entraining clastic material (including probably artefacts) and re-depositing it at close distance (see Karkanas et al., this volume).

The erosional event described above, and specifically the erosional contacts between the fossiliferous horizons in the two areas, provide the essential background for the analysis and interpretation of the spatial distributions at Marathousa 1.

The secondary deposition nature of the main find horizons raises the question of how reliable is the spatial association between the lithic artefacts and the partial skeleton of a single individual of *Elephas (Palaeoloxodon) antiquus* and the other faunal remains. Since spatial association does not necessarily imply causation, the answer has important consequences for the interpretation of the site in the broader context of the Middle Pleistocene human-proboscidean interactions. We aim to tackle this question and disentangle the formation processes acting at Marathousa 1 on the basis of spatial patterns through a three-prong spatial analytic approach:

1. by analysing, in a frame of references, the fabric of remains from relevant stratigraphic units;
2. by quantifying and comparing their relative vertical distributions;
3. by identifying spatial trends in either the assemblage intensities and the associations between classes of remains.

3. Material and methods

Since 2013, systematic investigation of the Marathousa 1 site has been carried out by a joint team from the Ephoreia of Palaeoanthropology-Speleology (Greek Ministry of Culture) and the University of Tübingen. A grid of 1 square meter units was set up, oriented -14 degrees off the magnetic North, and including the two areas of investigation. The excavation of the deposit proceeded into sub-squares of 50x50 cm in Area B and 1x1 m squares in Area A, and spits of about 5 to 10 cm thickness, respectively. Systematic screen-washing of sediments was carried out on-site using 1 mm sieves, in order to guarantee recovery of the small-size fraction (e.g., micro-artefacts, small mammal remains, fish, molluscs and small fragments of organic and inorganic material). The three-dimensional coordinates of finds (i.e., all the lithic artefacts, teeth and diagnostic bones; bones and organic material with a-axis ≥ 20 mm), collected spits of sediment, samples and geological features (e.g., erosional contacts and mud cracks)

were recorded with the use of a Total Station. The dimensions (length, width and thickness) of registered finds were measured on-site with millimetre rules. Orientation (dip and strike) of elongated particles (i.e., faunal remains, large wood fragments and lithic artefacts) was recorded since 2013 with a 30 degree accuracy, using a clock-like system (the strike was measured, relatively to the grid North, in twelve clockwise slices). In 2015, the use of a compass and inclinometer with an accuracy of 1 degrees was introduced in Area B to gradually replaced the former method. Strike (azimuth) and dip measurements were taken along the a-axis (symmetrical longitudinal axis) of the bones ([Domínguez-Rodrigo and García-Pérez, 2013](#)), the lithic artefacts ([Bertran and Texier, 1995](#)) and organic material, using the lowest endpoint of the axis as an indicator of the vector direction.

The present study focuses on the excavated stratigraphic units in which most of the archaeological and palaeontological remains were recovered in both excavation areas, namely UA3c and UA4 in Area A, and UB4c and UB5a in Area B. From the total, subset samples of material were used for each specific spatial analysis. For the fabric analysis we included material collected until 2016. For the vertical distribution and point pattern analyses, the region of investigation was limited to the squares excavated from 2013 until 2015, 25 and 29 square meters respectively in each area.

The analyses were performed in R statistical software ([R Core Team, 2016](#)). In order to make this research reproducible ([Marwick, 2017](#)), a repository containing a compendium of data, source code and text is open licensed available at the DOI: [10.5281/zenodo.822273](https://doi.org/10.5281/zenodo.822273)

3.1. Fabric analysis

Comparative fabric analysis was conducted with the aim to investigate the dynamics of the depositional processes at Marathousa 1. The analysis of the orientation of elongated clasts can distinguish three main types of pattern (isotropic, planar and linear fabric), each one associated with different sedimentary processes.

At the margin of a lacustrine environment, relatively close to the surrounding relief, a combination of high- and low-energy processes can be expected. According to the depositional context of the site (Karkanas et al., this volume), a strong preferred ori-

entation of clasts (linear pattern) would suggest the action of massive slope processes such as mudslides and debris / hyperconcentrated flows. On the other hand, whereas the frontal lobes of debris flows have been found to show a more random orientation (isotropic pattern), overland flows have been associated with planar fabrics ([Lenoble and Bertran, 2004](#)). Conversely, in a lacustrine floodplain, anisotropy without significant transport can be caused by low-energy processes such as lake transgression and regression, as well as water-sheet formed during rainy seasons. Isotropic patterns have been observed in different parts of mudflats as well ([Cobo-Sánchez et al., 2014](#)).

Nevertheless, grey zones exist between different depositional processes, so that an unequivocal discrimination based only on fabric observations is often not possible, and other taphonomic criteria must also be considered.

Since fabric strength has been found to be positively correlated with the shape and size of the clast, for the fabric analysis we subset samples of remains with length ≥ 2 cm and elongation index (the ratio length/width) $I_e \geq 1.6$ ([Lenoble and Bertran, 2004](#)). The samples are listed in Table 1 and include mostly wood fragments and faunal remains from the four stratigraphic units studied here. No distinction of skeletal elements was made, both due to the high fragmentation rate of faunal remains in Area B, and because recent experiments showed a similar orientation pattern for different bone shapes ([Domínguez-Rodrigo and García-Pérez, 2013](#); [Domínguez-Rodrigo et al., 2012](#)).

The sample of bones belonging to the individual of *Elephas (P.) antiquus* from Area A was analysed separately and included the humerus, ulna, femur and tibia; the atlas, axis and 16 complete vertebrae or vertebra fragments; 29 complete ribs or rib fragments; 2 calcanea; 4 metatarsals/metacarpals; the pyramidal; the trapezoid and the pelvis. The sample from UB5a was too small (only 7 observations) and was therefore excluded. The sample from the UB4c unit was divided in two sub-samples considered separately: those recorded using the clock method and those recorded using the compass method. All the sampled observations are representative of the whole area of interest.

Rose diagrams and uniformity tests, such as Rayleigh, Kuiper, Watson and Rao tests ([Jammalamadaka et al., 2001](#)), were used to visualise and evaluate circular isotropy

Table 1: List of sampled observations for the fabric analysis.

Sample	<i>n</i>	Type		
		Fauna	Wood	Lithic
UA3c	49	23	25	1
UA4	38	8	30	-
<i>E. (P.) antiquus</i>	63			
UB4c (clock)	86	68	4	14
UB4c (compass)	65	47	10	8

in the sample distribution. The Rayleigh test is used to assess the significance of the sample mean resultant length (\bar{R}), assuming that the distribution is unimodal and not bi- or plurimodal. The \bar{R} ranges from 0 to 1: values close to 1 indicate that the data are closely clustered around the mean direction; when the data are evenly spread \bar{R} has a value close to 0. A *p-value* lower than 0.05 rejects the hypothesis of randomness with a 95% confidence interval. Kuiper, Watson and Rao are omnibus tests used to detect multimodal departures from circular uniformity. All of them were applied using a significance level of *alpha* = 0.01. The test results were evaluated against critical values: a result higher than the critical value rejects the null hypothesis of isotropy with a 99% confidence interval.

Randomness testing of three-dimensional data was conducted with the Woodcock S_1/S_3 test (Woodcock and Naylor, 1983). Considering both the dip (plunge) and strike (bearing) of the oriented items, this method, based on three ordered eigenvalues (S_1 , S_2 , S_3), is able to discriminate the shape and strength of the distributions. The shape parameter $K = \frac{\ln(S_1/S_2)}{\ln(S_2/S_3)}$ ranges from zero (uni-axial girdles) to infinite (uni-axial clusters). The parameter $C = \ln(S_1/S_3)$ expresses the strength of the preferential orientation, and its significance is evaluated against critical values from simulated random samples of different sizes. A perfect random uniform distribution would have $C = 0$ and $K = 1$.

The Benn (Benn, 1994) diagram adds to the Woodcock test an isotropy ($IS = S_3/S_1$) and an elongation ($ES = 1 - (S_2/S_1)$) index. Like the former method, it is able to differentiate between linear (cluster), planar (girdle) or isotropic distributions.

There are no published raw data from actualistic studies on depositional processes affecting the orientation of bones and artefacts deposited on lacustrine floodplains (but see [Morton \(2004\)](#) and [Cobo-Sánchez et al. \(2014\)](#) as pioneer studies on this subject). However, we included in the Benn diagram references to published results from observation of fabrics in modern subaereal slope deposits ([Bertran et al., 1997](#); [Lenoble and Bertran, 2004](#)).

Fabric analysis is a powerful tool but, as suggested by [Lenoble and Bertran \(2004\)](#), it is not sufficient to unequivocally discriminate processes and should therefore be integrated with the analysis of other diagnostic features.

3.2. Vertical distribution

We provisionally assume that a general concentration of unsorted material in the proximity of the erosional surfaces would support an autochthonous origin of the assemblages; whereas a poorly to extremely poorly sorted and homogeneous vertical distribution of remains from the UA3c and UB4c units would suggest an allochthonous origin and a subsequent secondary deposition triggered by a massive process, e.g., debris or hyperconcentrated flows. Graded bedding could result in such fluid depositional environments, associated with a decrease in transport energy.

In order to estimate the degree of vertical dispersion while controlling for the size of the archaeological material, dimensional classes were set up following typological criteria. Lithic artefacts were classified as debris/chip when smaller than a cutoff length of 15 mm (see Tourloukis et al., this volume). Other classes include flakes, tools and cores; the latter being the bigger and heavier debitage product. Table 2 summarises the sample size for each class. Lithic debris/chips constitutes the larger part of the assemblages from UB4c (60%) and UB5a (49%); whereas in Area A it represents only a moderate percentage in the upper UA3c unit (16%). The very rare presence of lithic artefacts in the underlying unit UA4 is nevertheless significant. In this unit, the faunal remains are also found in much lower numbers, their number reduced to one fourth of those found in UA3c. For the point pattern analysis (see below), we used the same subset of materials for both excavation areas.

Table 2: List of sampled observations for the vertical distribution and point pattern analyses.

Sample	<i>n</i>	Lithic class					Faunal class			
		Debris/chip	Flake	Bone flake	Tool	Core	Indet.	Bone	Tooth	Microfauna
UA3c	279	46	2	-	1	-	1	171	14	44
UA4	61	3	1	-	-	-	-	45	4	8
UB4c	1243	753	154	1	34	6	2	246	28	19
UB5a	101	50	12	-	3	-	-	30	3	3

For Area B, the material recovered from the water-screening was randomly provenanced according to the 5 cm depth of the excavated spit and the coordinates of the 50x50 cm quadrant of the excavation square. Following the same excavation protocol, the same procedure was applied for the water-screened material of Area A, which was randomly provenanced according to 3D-coordinates of the 1x1 m excavation square and 10 cm spit.

Inverse-distance weighting (IDW) interpolation of the recorded points of contact between the UB4c/5a and UA3c/4 stratigraphic units were used to reconstruct their erosional surfaces, in Areas A and B, respectively (Fig. 3a,b). IDW assumes spatial autocorrelation and calculates, from a set of irregular known points, weighted average values of unknown points. Thus, in order to address our specific objective, i.e., to quantify and analyse the vertical distribution of the archaeological and palaeontological material, we measured the minimum orthogonal distance of each specimen to the interpolated erosional surface (Fig. 3c).

For the units above and below this surface (i.e., UB4c and UB5a), the relative distribution of lithic classes and faunal remains was informally tested by means of kernel density estimations. Likewise, in Area A the relative vertical distribution of remains from UA3c was estimated relative to the absolute elevation of the elephant remains and the range of elevations of the UA3c/4 surface. Finally, a Student's two sample t-test allowed us to compare the empirical distributions of different groups of remains for each stratigraphic unit.

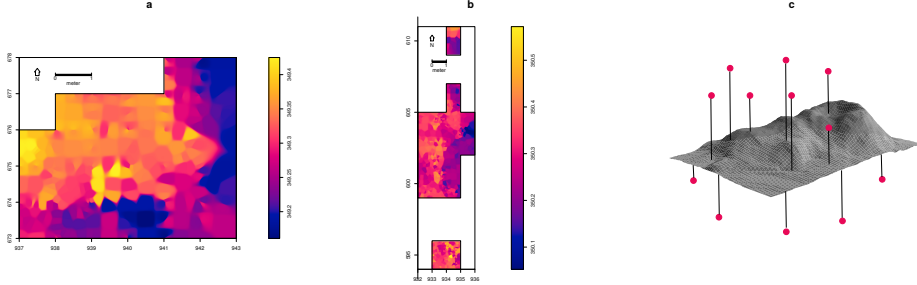


Figure 3: IDW interpolation of the UA3c/4 (a) and UB4c/5a (b) points of erosional contact; the color scale denotes elevation a.s.l. Illustration of the method used to quantify the vertical dispersion of remains with respect to the UB4c/5a surface (c).

3.3. Point pattern analysis

A spatial point pattern is defined as the outcome of a random spatial point process (repetitions of it would always create a different pattern). The observed patterns of the archaeological and palaeontological remains were treated as manifestations of spatial point processes, i.e., site formation processes. Point pattern analysis investigates the spatial arrangement of points with the aim to identify spatial trends. In order to integrate the previous studies of the fabric and vertical distributions, we directed our point pattern analysis equally to the intensity of the patterns (the rate of occurrence of the recorded finds) and to the spatial interaction between different types of finds.

As the average number of random points per unit area, intensity informs about homogeneity or inhomogeneity in the distribution of events generated by a point process, i.e., whether the rate of occurrence is uniform or spatially varying across the study area. Intensity, usually non-parametrically evaluated by means of kernel density estimation ([Diggle, 1985](#)), was assessed for the distribution of material from the UB4c, UB5a and UA3c units. Cross-validation bandwidth, which assumes a Cox process, and edge correction were applied using the methods described in [Diggle \(1985\)](#).

In the presence of a covariate, it is recommended to further investigate the dependence of intensity on that explanatory variable. In order to evaluate whether variation in the density of materials was correlated to the topography of the erosional surface, we computed a local likelihood smoothing estimate of the intensity of remains from

UB4c as a function of the UB4c/5a surface elevation model (Baddeley et al., 2012). Formal tests enabled us to assess the evidence of that dependence and to quantify the strength of the covariate. The Kolmogorov-Smirnov test of CSR (Complete Spatial Randomness) and Berman's Z_2 statistics were used to test the strength of evidence for a covariate effect. The Receiver Operating Characteristic (ROC) plot, and the area under the ROC curve (AUC), closely related to Berman's Z_2 test, measure the magnitude of the covariate effect. AUC values close to 1 or 0 indicate strong discrimination, whereas intermediate values (0.5) suggest no discrimination power.

Whereas intensity is a first-order property of the point process, multiscale inter-point interaction is measured by second or higher-order moment quantities, such as the Ripley's K correlation function (Ripley, 1976, 1977) and the distance G -, F - and J -functions. Three different types of inter-point interaction are possible: random, regular or cluster. Regular patterns are assumed to be the result of inhibition processes, while cluster patterns are the result of attraction processes. In order to reduce the edge effect bias in estimating the correlation between points, we implemented Ripley's isotropic edge correction (Ohser, 1983; Ripley, 1988). In a hypothesis-testing framework, pointwise envelopes were computed by 199 random simulations of the null hypothesis. Thus, values of the empirical distribution (black solid line) were plotted against the benchmark value (red dotted line) and the envelopes (grey area) which specify the critical points for a Monte Carlo test (Ripley, 1981).

In order to test the spatial dependence between remains associated with the erosional event of UB4c and those associated with the underlying UB5a unit, we treated the data as a multivariate point pattern, assuming that the point patterns in UB4c and UB5a are expressions of two different stationary point processes, i.e., depositional events. We performed a cross-type pair correlation function ($g_{ij}(r)$), derivative of the multitype $K_{ij}(r)$ function, which is the expected number of points of type j lying at a distance r of a typical point of type i . The function is a multiscale measurement of the spatial dependence between types i (UB4c) and j (UB5a). Randomly shifting each of the two patterns, independently of each other, estimated values of $\hat{g}_{ij}(r)$ are compared to a benchmark value $g_{ij}(r) = 1$, which is consistent with independence or at least with lack of correlation between the two point processes.

In addition to the pair correlation function, the multitype nearest-neighbour $G_{ij}(r)$ function was used to estimate the cumulative distribution of the distance from a point of type i (UB4c) to the nearest point of type j (UB5a). It measures the spatial association between the two assemblages. For the cross-type G -function, the null hypothesis states that the points of type j follow a Poisson (random) distribution in addition to being independent of the points of type i . Thus, in a randomisation technique, when the solid line of the observed distribution ($\hat{G}_{ij}(r)$) is above or below the shaded grey area, the pattern is significantly consistent with clustering or segregation, respectively. Complete spatial randomness and independence (CSRI) of the two point processes would support an exogenous origin hypothesis for the assemblage recovered from the UB4c unit. On the other hand, positive or negative association can be interpreted as expression of different endogenous processes.

The particle size spatial distribution of the lithic assemblage from UB4c was investigated by means of a transformation of the multitype K -function ($K_{i\bullet}(r) - K(r)$, see [Baddeley et al. \(2015\)](#), p.608). In this case, we treated the data as the manifestation of a single multitype point process. In a joint distribution analysis, the locations and types of points are assumed to be generated at the same time. The null model of a random labelling test states that the type of each point is determined at random, independently of other points, with fixed probabilities. The estimated K -function for a subset of possible combinations was evaluated against the envelope of Monte Carlo permutations of the class of remains. Likewise with the vertical distribution, a horizontal clustering of small specimens, such as lithic debris/chips, together with larger dimensional classes of remains would suggest the lack of sorting by natural depositional processes and a *en masse* model of deposition.

As for the three-dimensional distribution of the lithic artefacts in Area A, and their spatial association with the partial skeleton of the *E. (P.) antiquus*, we applied three-dimensional univariate and bivariate second-order functions. A rectangular box of 20 square meters and 80 cm vertical extent was selected for the analyses (green outline in Fig. 9a). Assuming homogeneity, the univariate pair correlation function ($g_3(r)$) was estimated for the pattern of all the artefacts (mostly debris/chips) from UA3c and UA4. In the specific context of the site, complete spatial randomness (CSR) would suggest

Table 3: Global tests for circular uniformity

Sample	mean dir.	Rayleigh		Kuiper		Watson		Rao		level
		\bar{R}	p - value	test	critical value	test	critical value	test	critical value	
UA3c	77.17°	0.268	0.029	2.4698	2.001	0.2967	0.267	271.8367	160.53	0.01
UA4	35.79°	0.386	0.003	2.5656	2.001	0.3437	0.267	246.3158	163.73	0.01
<i>E. (P.) antiquus</i>	54.64°	0.489	2.775e-07	3.4811	2.001	0.906	0.267	291.4286	155.49	0.01
UB4c (clock)	83.96°	0.167	0.091	2.327	2.001	0.2466	0.267	309.7674	155.49	0.01
UB4c (compass)	128.14°	0.225	0.037	1.6917	2.001	0.1862	0.267	153.3846	155.49	0.01

that the pattern most probably is the result of a random distribution process, such as a high energy mass movement. In contrast, other natural processes would produce clustering or segregation of the lithic artefacts. Spatial aggregation, if not generated by obstructions, would support an *in situ* primary origin of the assemblage.

In support to the pair correlation function, the cross-type nearest-neighbour function has been applied in order to compute, for each artefact recovered from the UA3c and UA4 units, the nearest point associated with the elephant skeleton. A prevalence of short distances would indicate aggregation of the lithic artefacts around the mass of the elephant; whereas a uniform or symmetric distribution would support random independent processes.

4. Results

4.1. Fabric analysis

The rose diagrams in Fig. 4 visualise the circular distributions of the examined specimens. Overall, the UA4 sample and the sample of elephant bones show predominant peaks in the NE quadrant; while the ones from units UA3c and UB4c suggest uniform to multimodal distributions. Specifically, the UA4 sample distribution (Fig. 4b) spreads largely in the NE quadrant. Similarly, the circular distribution of the elephant sample (Fig. 4c), mainly lying in UA4, resembles the former distribution: it is skewed to the SW and concentrated in the NE quadrant. On the other hand, the UA3c sample (Fig. 4a) and the two samples from Area B (Fig. 4d,e) suggest a different isotropic scenario.

Table 3 summarises the results of the circular uniformity tests. With regard to the UA3c sample, the Rayleigh test ($p - value = 0.029$) rejected the null hypothesis of

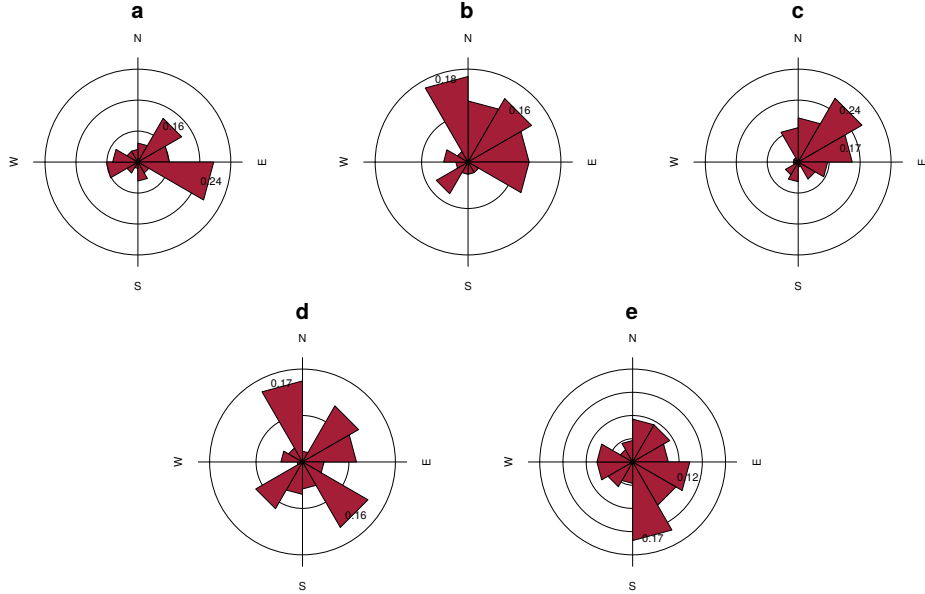


Figure 4: Rose diagrams showing the bearing patterns of samples from UA3c (a), UA4 (b), the elephant carcass (c) and UB4c (d: clock method, e: compass method)

circular uniformity. The mean resultant length ($\bar{R} = 0.268$) and the mean direction of 77.17° are thus significant, assuming the distribution is unimodal. However, the Kuiper, Watson and Rao omnibus tests also rejected the null hypothesis of uniformity, therefore suggesting multimodal anisotropy in the distribution, as shown by the rose diagram (Fig. 4a).

For the UA4 sample and the subset of elephant bones, all the tests agreed in rejecting the null hypothesis in favour of a preferentially oriented distribution. The Elephant sample, with respect to the other, showed stronger anisotropy and significantly higher \bar{R} . As suggested by the rose diagrams (Fig. 4c), this sample has a mean direction towards the NE (55°) and relatively low circular variance (29°).

The UB4c sub-samples had discordant test results when considering the Rayleigh and the omnibus statistics. According to the Rayleigh test, the mean resultant length (\bar{R}) and the mean direction were not significant for the sub-sample of measurements recorded with the clock system. Conversely, a weak significant test result was obtained for the sub-sample of measurements recorded using the compass. Overall, for the latter

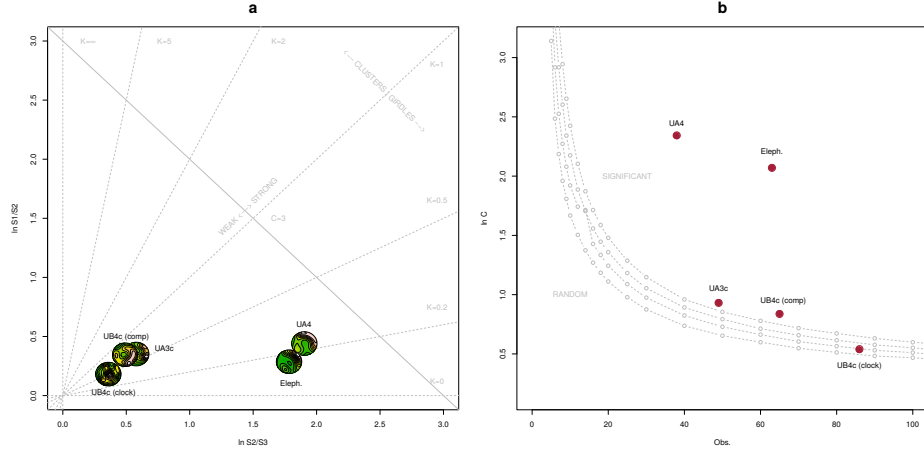


Figure 5: Woodcock's eigenvalues ratio graph (a) and plot of the Monte-Carlo critical S_1/S_3 test values, for varying sample sizes and confidence levels (b), modified from [Woodcock and Naylor \(1983\)](#).

sub-sample all the omnibus tests suggested significant isotropy (Fig. 4e). On the other hand, the Kuiper and Rao tests, suggested a multimodal departure from uniformity for the sample recorded using the clock method (Fig. 4d).

The results obtained for the UA3c sample and the UB4c sub-sample recorded using the clock method are most probably due to the shape of those distributions. Indeed, the clock system, being less accurate, tends to produce a less dense distribution, more subject to show a multimodal shape when the distribution is actually uniform (Fig. 4a, d).

The Woodcock eigenvalues ratio graph (Fig. 5a) presents the shape (K) and strength (C) of the distributions. Fig. 5b plots confidence levels of Monte-Carlo critical C values, varying for sample sizes. The two samples from Area B, together with the UA3c sample, having low C values, plotted close to the origin of the ratio graph. Thus, they suggest nearly significant randomness. On the other hand, the UA4 and the elephant samples, with higher C values, showed a stronger and significant tendency to orient preferentially. The shape parameter K of the samples varied from $K = 0.7$ for the UB4c sample measured with the compass to $K = 0.1$ for the elephant sample. Overall, all the samples plotted below the average shape value ($K = 1$) between girdles and clusters distributions.

The Benn diagram (Fig. 6) resembles the Woodcock ratio graph (Fig. 5a). The samples from units UB4c and UA3c clearly plotted at a distance from the UA4 and the elephant samples. The UB4c sub-sample of measurements recorded with the compass, together with the UA3c sample, plotted in the centre of the ternary graph. As shown above, the UB4c sub-sample of measurements taken using the clock system exhibited more isotropy.

Compared to the ranges recorded for modern natural processes (debris flow, runoff, solifluction), the fabric from the UA3c and UB4c units plotted well inside the cluster of debris flows, with the UB4c (clock) sample suggesting even more random orientations. On the other hand, the sample of elephant remains, which lie mostly on UA4 and are covered by UA3c, plotted significantly close to the sample from unit UA4. They both presented the lowest isotropy index (*IS*), but not high elongation index (*EL*). Thus, they plotted in the average between linear and planar orientations, within the range of runoff processes. Yet they still plotted at the margins of the cluster of debris flows fabrics. Moreover, the elephant sample showed a more planar attitude with respect to the UA4 sample.

4.2. Vertical distribution

Fig. 7 compares the distribution of the absolute elevations of the partial skeleton of the *Elephas (P.) antiquus* with the other remains from Area A. Overall, the vertical distribution of the elephant approximates a normal distribution with mean (μ) 349.25 m a.s.l. and standard deviation (σ) 0.12 m. The mean elevation of the erosional contact between the two stratigraphic units is slightly above the latter ($\mu = 349.30$ m). Although difficult to quantify due to its not sharp nature, the range of elevations of this contact, as estimated from the IDW interpolation (Fig. 3a), is relatively small ($\sigma = 0.06$ m).

Three lithic artefacts (two flakes and one tool) from the UA3c unit are located within its positive half. Only one flake has been found in the lower UA4, at about 349.10 m, together with three chips. However, they plotted well within the left tail of the debris/chip distribution from the unit above. Despite the scarcity ofdebitage products in this area, waste products (debris/chip) are relatively well represented (16%

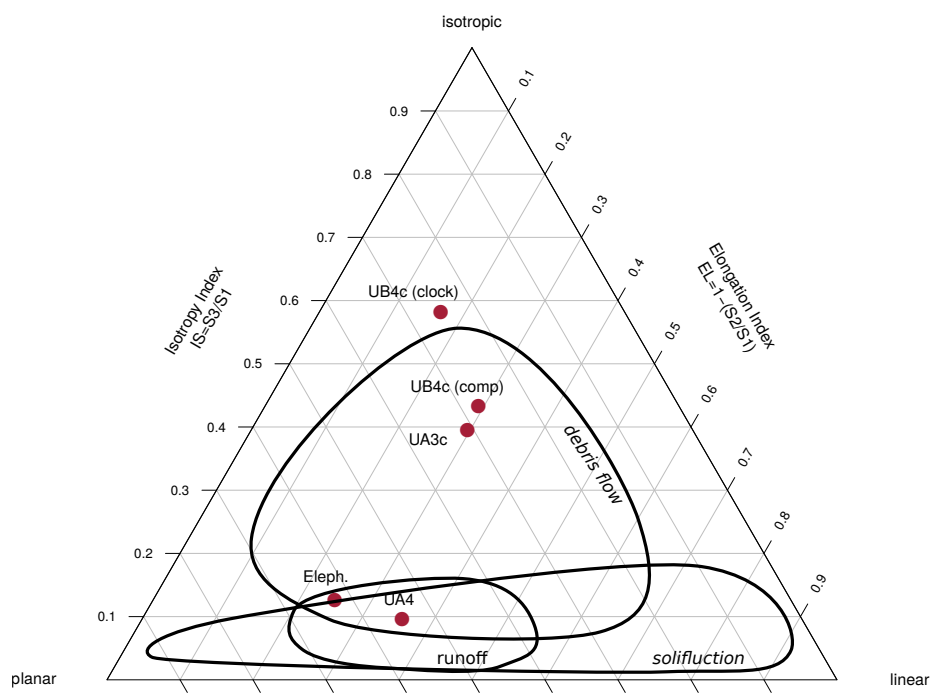


Figure 6: Benn's diagram. Fabric ranges of natural processes modified from Bertran et al. (1997); Lenoble and Bertran (2004).

of the UA3c sample). Their vertical distribution approximates a normal distribution ($\mu = 349.50$ m and $\sigma = 0.18$ m), having almost 50% of the sample in the range of elevations of the erosional surface and the rest above it. Notably, the distribution of the faunal remains from the same unit resembles that of the debris/chip. The Welch two sample t-test ($p - value = 0.5099$) failed to reject the null hypothesis that the two population means are equal. On the other hand, the vertical distribution of faunal remains recovered from the UA4 unit is comparable with that of the *Elephas* ($p - value = 0.6562$). Nevertheless, the density functions altogether clearly confirm one of the main observations assessed during excavation, namely that the elephant remains and most of the recovered faunal and lithic material in Area A lie at or close to the UA3c/4 contact, with unit UA3c covering the remains.

Fig. 8 shows the empirical density functions of the minimum distances from each specimen from Area B to the UB4c/5a erosional contact (Fig. 3b). The combined distribution of any type of find from the UB5a unit (Fig. 8a) skewed to the left with a short tail (up to -0.3 m). The mode, between 5 and 10 cm below the roof of UB5a, indicates a general concentration of material very close to the contact of this unit with the overlying UB4c, in accordance with the mean distribution of the different classes of remains. Although the majority of both the lithic and faunal assemblages were found in the uppermost 15 cm of UB5a, few debris/chips and bone fragments occur lower in the sequence, yet no more than 30 cm below the roof of this unit. Very few flakes, three tools and no cores have been found in this unit. As a whole, the lithic assemblage from UB5a, mostly composed by debris/chips, is only 7% of the most conspicuous assemblage from UB4c.

The global distribution of unit UB4c was right skewed (up to almost 0.6 m) and centred at about 5 cm above the contact with the underlying unit UB5a (Fig. 8b). Almost 30% of the sample fell exactly at the erosional contact that separates UB4c from UB5a. The density estimations of the lithic debris/chip, flakes, tools and faunal remains significantly overlap, whereas the distribution of the six cores shows a bimodal shape with peaks at 5 and 20 cm above the contact. However, the Welch Two Sample t-test of the lithic and faunal sample means failed to reject the null hypothesis ($p - value = 0.6295$).

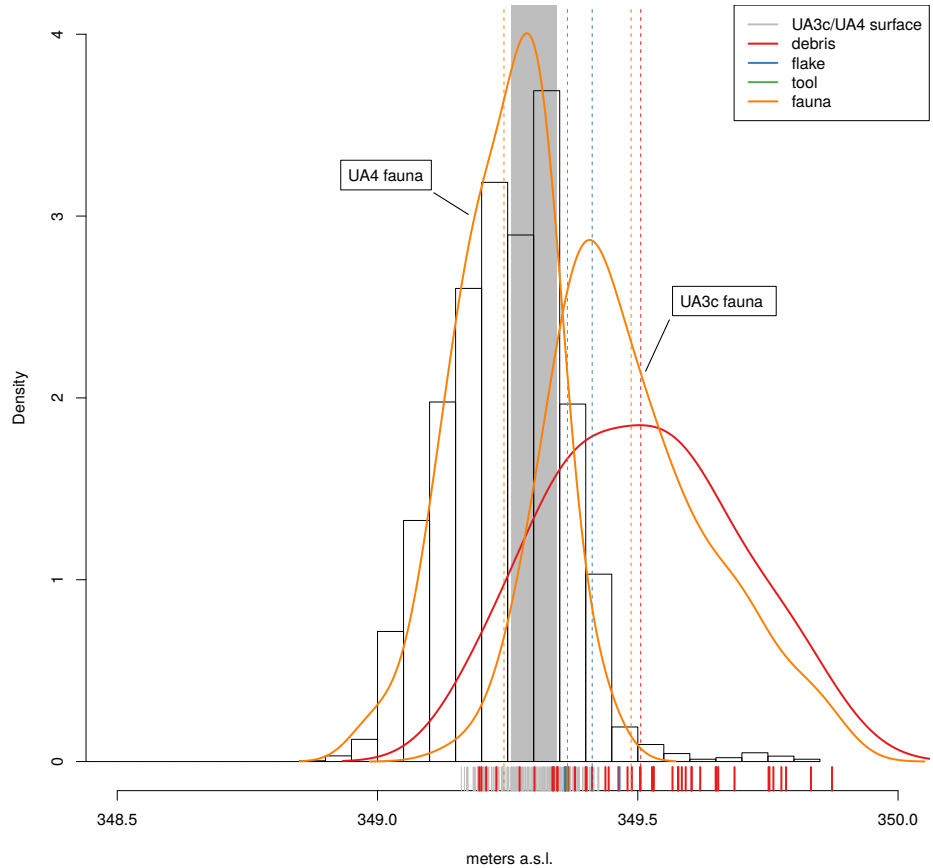


Figure 7: Empirical density functions of absolute elevations (meters a.s.l) of remains from Area A. The histogram represents the *Elephas (P.) antiquus* range of elevations; the grey area shades the $Q_3 - Q_1$ range of the erosional UA3c/4 surface; dashed lines indicate mean values.

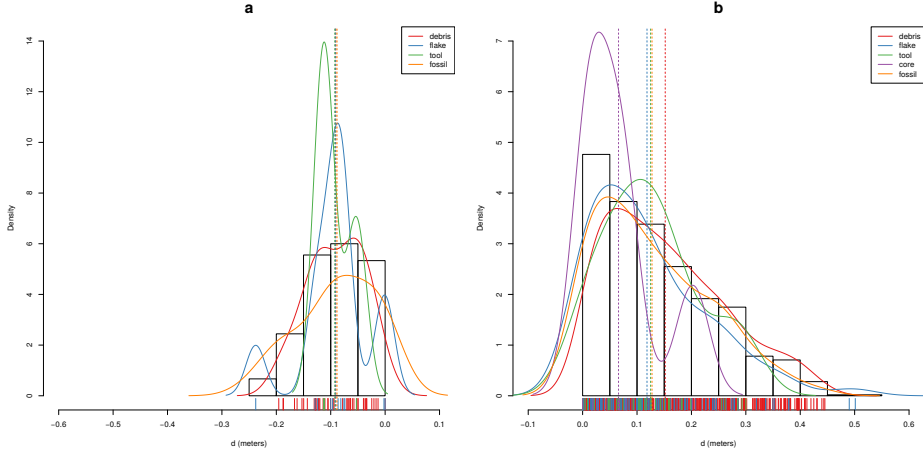


Figure 8: Empirical density functions of minimum orthogonal distances (d) to the UB4c/5a surface. The histogram represents the total distribution of remains from UB5a (a) and UB4c (b); dashed lines indicate mean values.

4.3. Point pattern analysis

Results of the point pattern analysis are complementary to those obtained from the analysis of the vertical and fabric distributions.

Regarding Area A, kernel density estimation and three-dimensional functions were applied in order to quantitatively depict the spatial distribution of the lithic assemblage in relation to the elephant skeleton.

Fig. 9a shows the smoothing kernel intensity estimation of the combined lithic and faunal assemblage from the UA3c unit. Contour lines delimit the density of the lithic sample. The partial skeleton of the *E. (P.) antiquus* is superimposed on it. A preliminary visual examination of the plot suggests a homogeneous distribution of lithics (mostly debris/chips) and fossils. Spots of higher density appear to be spread around and in association with the elephant remains.

The univariate pair correlation function of the joined lithic assemblage from the UA3c and UA4 units (Fig. 9b) suggests aggregation of finds. The estimated $\hat{g}_3(r)$ function (black solid line) wanders above the benchmark value (red dotted line) until values of $r = 0.8$. However, for distances between 35 and 65 cm, it lies above the grey envelope of significance for the null hypothesis of CSR, indicating that at those

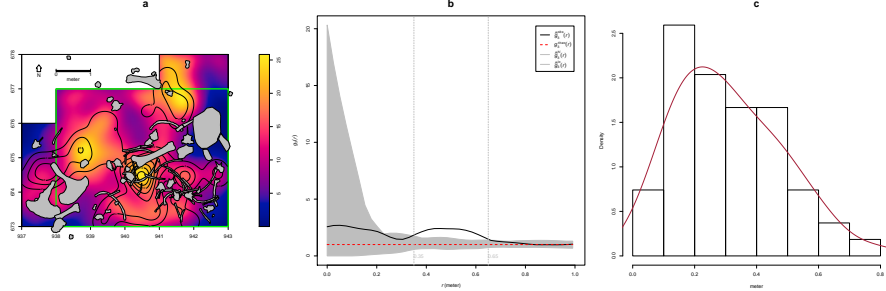


Figure 9: Kernel smoothed intensity function of the lithic and faunal assemblages from UA3c. Isolines mark the density of the lithic artefacts (a). Pair correlation function ($g_3(r)$) of a three-dimensional pattern of lithic artefacts from UA3c and UA4. Grey envelope of 999 Monte Carlo simulations under the CSR null hypothesis (b). Three-dimensional distance from each lithic artefact from UA3c and UA4 to the nearest neighbour elephant remain (c).

distances artefacts occur closer than expected in the case of random processes. For values of $r > 0.8$, the function stabilises at values close to 0, suggesting a Poisson distribution. The plot illustrates the random distribution of finds between patches of clusters that we observe in the kernel density estimation (Fig. 9a).

The histogram in Fig. 9c shows the density of the distances calculated from each artefact to the nearest-neighbour elephant remain. A right skewed distribution, with a prevalent peak at 10 cm and mean μ 30 cm is an indication of the relatively strong aggregation of events around the mass of the elephant skeleton.

As for Area B, the analysis first focused on the spatial distribution and cross-correlation of the assemblages from UB4c and UB5a (Fig. 10); and secondly on the interaction between classes of remains from UB4c (Fig. 11).

Figs. 10a,b respectively show kernel density estimations of the combined lithic and faunal assemblages from both the units analysed. Despite the samples size difference, a first visual examination suggests the presence of interesting spatial structures.

Regarding the UB4c unit (Fig. 10a), the high density of material concentrated around the western square 934/600 suggests that the pattern could have been the result of an inhomogeneous, non-uniform depositional process. Visual comparison of the density plot with the elevation model of the erosional contact between the UB4c

and UB5a units (Fig. 3b) suggests positive correlation between lower elevations (topographic depressions) and higher density of remains. Fig. 10c shows the results of the ρ -function, which estimates the intensity of the UB4c sample assemblage as a function of the covariate underlying topography created by the erosional event. Within the range of elevation between 350.2 and 350.4 m, the occurrence of finds is higher and the intensity decreases with the rise of elevation, i.e., finds are more likely to be found at lower elevations than would be expected if the intensity was constant.

Spatial Kolmogorov-Smirnov and Berman's Z_2 (Berman, 1986) statistics were used in order to test the dependence of the UB4c pattern on the covariate erosional surface. Both KS ($D = 0.11952$, $p - value = 7.772e - 16$) and Z_2 ($Z2 = -7.8447$, $p - value = 4.34e - 15$) significantly rejected the null hypothesis of CSR. Although the tests suggested evidence that the intensity depends on the covariate, the effect of the covariate is weak and it seems to have no discriminatory power. The ROC curve and AUC statistics (0.56), which measure the strength of the covariate effect, suggest that the underlying UB4c/5a topography does not completely explain the localised high density of occurrence in the UB4c.

Relative spatial segregation seems to occur between the assemblages from UB4c (Fig. 10a) and UB5a (Fig. 10b), with high density of the former distribution corresponding to low density of the latter. The former analysis of the vertical distribution showed that the two assemblages occur very close to their stratigraphic contact. In order to further investigate the spatial interaction between the two depositional events, we applied multitype pair correlation ($g_{ij}(r)$) and nearest-neighbour ($G_{ij}(r)$) functions.

Fig. 10d shows the estimated values of the multivariate $\hat{g}_{ij}(r)$ function against the envelope of the null hypothesis, obtained by randomly shifting the position of remains from the two distributions in 199 Monte Carlo simulations. For fixed values of r less than 30 cm the observed function lies below the benchmark value of independence, thus indicating segregation; but it wanders at the lower edge of the grey envelope. For fixed distances of $r > 0.3$ m the observed and theoretical lines significantly overlap. Overall, the function suggests independence of the two point processes (UB4c and UB5a) at multiple scales.

However, the estimated $\hat{G}_{ij}(r)$ function (Fig. 10c), running well below the signifi-

cance grey envelope for fixed values of $r > 0.3$ m, confirms that the nearest-neighbour distances between remains from UB4c and UB5a are significantly longer than expected in the case of independent processes. Interestingly, at values of $r < 0.2$ m the observed function failed to reject the null hypothesis of Complete Spatial Randomness and Independence (CSRI).

With the aim to integrate the vertical distribution analysis, the particle size spatial distribution of remains from the UB4c unit were investigated by means of a derivative of the multitype K -function, randomly labelling the classes of remains. Fig.11 shows a selection of the array of possible combinations between classes. In any panel, the estimated function wanders above the benchmark value. Such positive deviations from the null hypotheses suggest that debris/chips are more likely to be found close to the other class of remains than would be expected in case of a completely random distribution. Permutating the lithic debris/chips with flakes (Fig.11a), tools (Fig.11b), cores (Fig.11c) and faunal remains (Fig.11d), the Monte Carlo test results would have been significantly consistent with clustering, if we had chosen distance values $r > 0.4$, $r > 0.4$, $r > 0.9$, $r > 0.8$, respectively. Conversely, we could not reject the null hypothesis of CSRI for lesser values of r .

5. Discussion

Recent excavations at the Middle Pleistocene site of Marathousa 1 have unearthed in one of the two investigated areas (Area A) a partial skeleton of a single individual of *Elephas (P.) antiquus*, whose bones are in close anatomical association, and spatially and stratigraphically associated with lithic artefacts and other faunal remains. In Area B, about 60 m to the South of Area A, we collected a much higher number of lithic artefacts (Tourloukis et al., this volume), spatially and stratigraphically associated with other faunal remains, including isolated elephant bones, cervids and carnivores among others (Konidaris et al., this volume).

The two areas are stratigraphically correlated, the main fossiliferous layers (UA3c and UB4c) representing a relatively low-energy depositional process, such as a hyper-concentrated flow that dumped material in a lake margin context (Karkanas et al., this

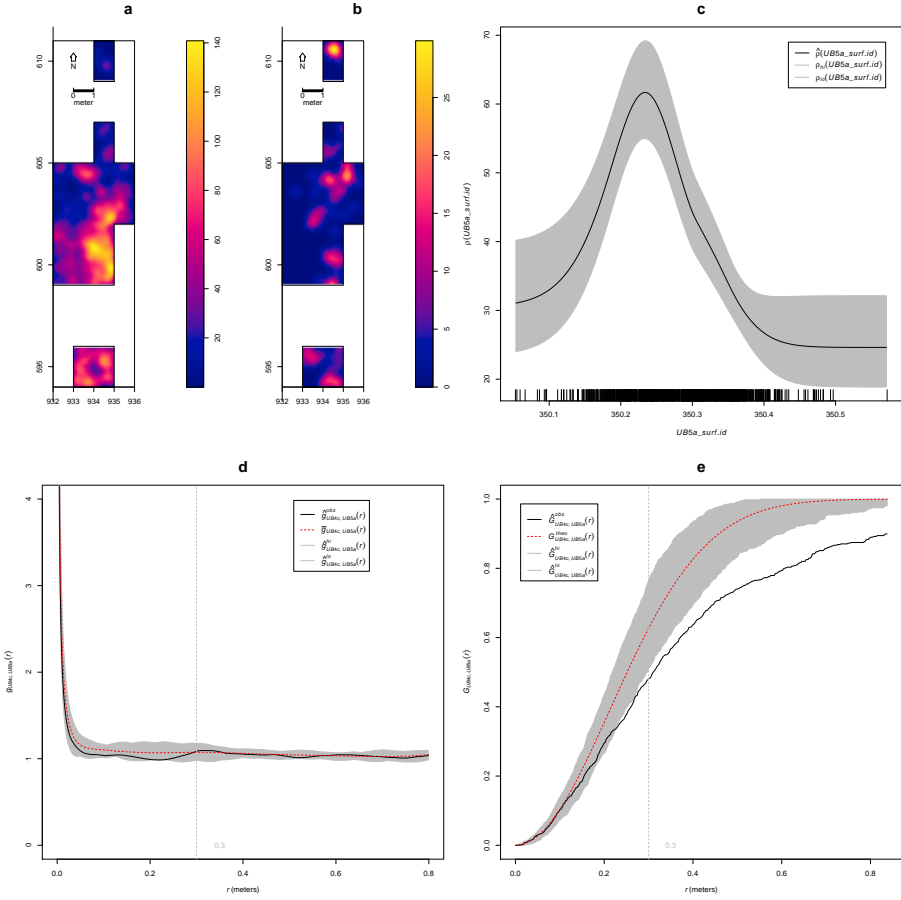


Figure 10: Kernel smoothed intensity function of the lithic and faunal assemblages from UB4c (a) and UB5a (b). Smoothing estimate of the intensity of remains from UB4c, as a function of the erosional surface UB4c/5a. Grey shading is pointwise 95% confidence bands (c). Cross-pattern pair correlation function ($g_{ij}(r)$) between the UB4c and UB5a distributions. Grey envelope of 199 Monte Carlo simulations under the independence of components null hypothesis (d). Multitype nearest-neighbour function ($G_{ij}(r)$) between the UB4c and UB5a distributions (e).

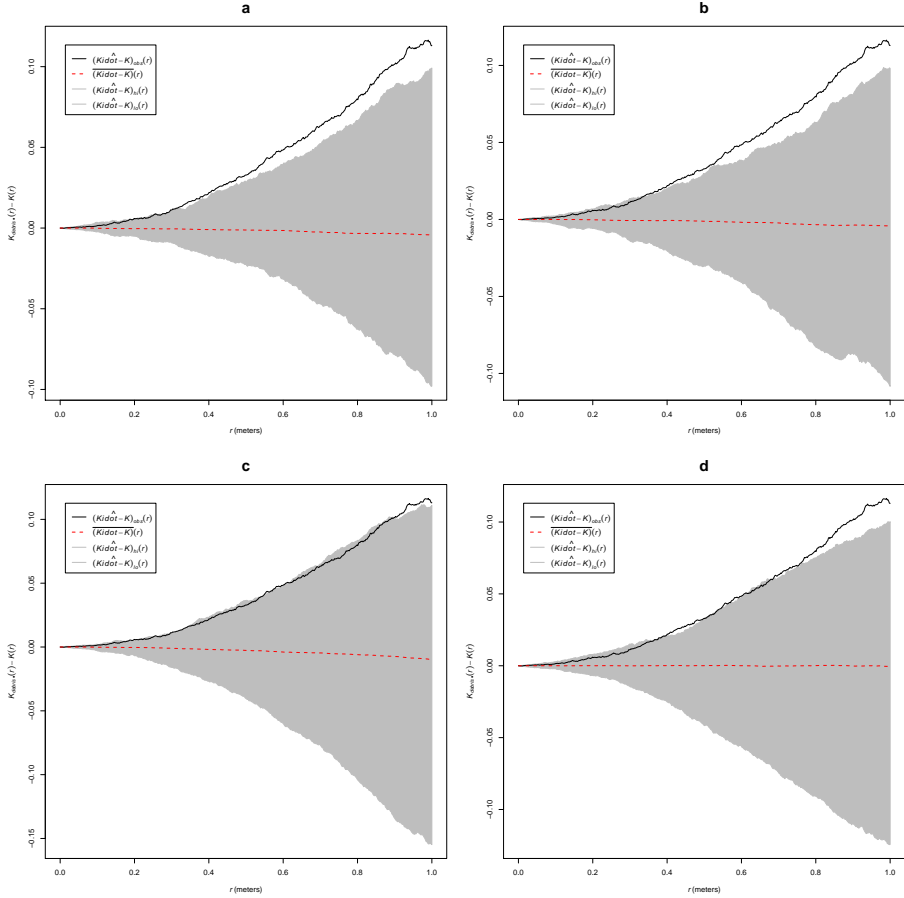


Figure 11: Random labelling test for the UB4c assemblage. Grey pointwise envelope of 199 Monte Carlo permutation of debris/chips with flakes (a); tools (b); cores (c); fossils (d).

volume).

To date, evidence of butchering (cut-marks) has been identified on two bones of the elephant skeleton from Area A, as well on elephant and other mammal bones from Area B (see Konidaris, this volume).

However, due to the secondary deposition nature of the main fossiliferous horizon, it is of primary importance to evaluate the degree and reliability of the spatial association of the lithic artefacts with the faunal remains, and especially with the elephant skeleton. In order to tackle our main objective, we applied a comprehensive set of spatial statistics to the distributions of the archaeological and zooarchaeological/palaeontological remains from relevant stratigraphic units of the two areas of investigation. Preliminary results are here discussed for both areas.

5.1. Fabric analysis

The analysis of the orientation (dip and strike) of subsets of remains, mostly bone fragments, organic residues and lithic artefacts, showed different patterns for the two main find-bearing units.

The test results (Tab. 3) for the UA4 sample and the sample of elephant remains - which lie on unit UA4 and are covered by UA3c - indicated significant preferential orientations towards the NE (Figs. 4b,c). As shown by the Woodcock's (Fig. 5) and the Benn's diagrams (Fig. 6), these samples plotted together at a distance from the others. Such convergence suggests that the elephant carcass, the other faunal remains and the organic material, deposited on unit UA4, were subjected to the same processes.

Far from the isotropic corner in the Benn's diagram these two samples from Area A plotted almost in between the linear and planar extremes, with the elephant sample showing a more planar fabric. When the results published by Bertran et al. (1997) and Lenoble and Bertran (2004) from observations of fabrics in modern subaerial slope deposits were used as a reference, the two samples aggregated well within the cluster of runoff process. Yet they still plotted at the extreme margins of debris flow and relatively distant from the linear corner.

This result is consistent with the exposure of unit UA4 to overland water-laden processes that occurred before the flood event UA3/UB4 (Karkanas et al., this vol-

ume). Notably, the erosive nature of low-energy processes triggered by rain-water has been observed on lacustrine floodplains, and is associated with anisotropic patterns in autochthonous assemblages (Cobo-Sánchez et al., 2014; Domínguez-Rodrigo et al., 2014c; García-Moreno et al., 2016).

On the other hand, the fabric of the UA3c sample, being similar to those of the UB4c sub-samples (Figs. 5 and 6), supports the stratigraphic correlation between these units across the two investigated areas. The fabric analysis suggests that the UA3/UB4 process can be categorized as a flood event, which falls in the spectrum between debris and hyperconcentrated flow. Indeed, random distribution and orientation of clasts is expected for debris flows, except at flow margins, where preferential orientation and clusters of clasts have been observed (Pierson, 2005). Eventually, such flood would have had the power to significantly reorient elements of the elephant carcass and slightly displace them.

Unlike bones with a tubular shape (i.e., long bones), ribs and vertebrae are prone to orient preferentially under high energy processes, less likely under low energy processes (Domínguez-Rodrigo and García-Pérez, 2013; Domínguez-Rodrigo et al., 2014c). Interestingly, whereas some of the ribs share the same preferential orientation with the long bones, others are oriented NW/SE. However, a NW/SE orientation could be consistent with a prevalent NE direction of the flow (and vice-versa), since long bones could roll orthogonally to the flow direction (Voorhies, 1966).

On the other hand, a higher energy flood would lead to an under-representation of most cancellous grease-bearing bones, which are prone to be easily transported by water induced processes (Voorhies, 1966). Yet several carpal, tarsal, metapodials, phalanges, ribs and vertebrae are present and in close spatial association with the elephant cranium and other skeletal elements.

The presence of many of the skeletal elements suggests that the elephant carcass was not subjected to high energy processes. Thus, we can assume that relatively low energy overland flows slightly reworked and oriented the exposed elements of the already dismembered (and probably already marginally displaced) elephant carcass, which mostly preserves close anatomical associations, but not anatomical connections.

In Area B, two sub-samples from the same stratigraphic unit were analysed, accord-

ing to the different methods used for recording the orientation (dip and strike) of the finds (i.e., 'clock' vs. compass), mostly faunal remains, wood fragments and lithic artefacts. Due to the different shapes of the two distributions (Figs. 4d,e), test statistics reported contrasting results (Tab. 3). Indeed, the clock system, recording non-continuous circular data, tends to produce a distribution more subject to show a multimodal shape when the distribution is actually uniform. However, the three-dimensional Woodcock (Fig. 5) and Benn (Fig. 6) diagrams agreed upon assessing the randomness of the samples. Despite minor differences between the two samples, both plotted with the UA3c sample in the reference range of debris flows.

5.2. Vertical distribution

As for the vertical distribution, we assume that mass wasting processes, such as debris or hyperconcentrated flows, would predominantly distribute extremely poorly sorted clasts homogeneously throughout the sequence. Normal or inverse grading can be observed in such flows (Pierson, 2005). A concentration of unsorted elements in the proximity of the erosional surface, as well as the absence of any grading, would in turn suggest an autochthonous assemblage.

The lithic assemblage from Area A - the combined sample from units UA3c and UA4 ($n = 54$), composed by a fewdebitage products and a relatively high number of debris/chips and retouch waste products (Tab. 2) - plotted predominantly in the proximity of the erosional surface created by the UA3/UB4 event. The faunal remains from unit UA3c resemble the distribution of the archaeological assemblage as a whole; whereas the ones from the underlying unit UA4 match the vertical distribution of the elephant (Fig. 7).

Overall, the material recovered from unit UA3c did not show any grading and mainly plotted at the bottom of the unit, thus consistent with the hypothesis of an autochthonous assemblage.

In Area B, two samples from units UB4c ($n = 1243$) and UB5a ($n = 101$) respectively, were analysed (Tab. 2), for quantifying the minimum orthogonal distance of each item to the modelled erosional surface (Fig. 3b).

The vertical distribution of lithic artefacts and fossils from unit UB4c showed a predominant peak right at the contact with the erosional surface. Almost 30% of this rich sample plotted at a distance between 0 and 5 cm from the erosional contact; whereas the rest gently skewed to the upper part of the unit, up to about 50 cm. The same distribution was observed for all classes of remains, suggesting no size sorting and an origin very close to the erosional surface (Fig. 8b).

The density distribution of the sample from the underlying UB5a unit (Fig. 8a) globally indicates a more constrained vertical displacement of remains (within 30 cm below the erosional surface). Whereas lithic artefacts and fossils mostly plot right at the contact and just below it, a few debris/chips and faunal remains were found lower in the sequence. No size sorting was observed, but, notably, lithic cores are absent and the debris/chip distribution is wider than the distribution of the few flakes and tools.

Field observations of cracks in the clayey UB5a unit testify shrinking and swelling during wetting and drying cycles (Karkanas et al., this volume), which suggests that vertical displacement of some small lithics and fossil fragments at lower depths with respect to the UB5a/4c contact probably resulted from clay desiccation.

Likewise, [Lenoble and Bertran \(2004\)](#) documented up to 30 cm vertical dispersion and frequent vertical dip of artefacts from the marshy silty clay of the Croix-de-Canard site, sector 3.

Furthermore, a recent experimental study of animal trampling in water saturated substrates reported negative correlation with artefact size, significant inclination and greater vertical displacement than any former work: a maximum between 16 and 21 cm, with a mean of about 6 cm ([Eren et al., 2010](#)).

The fact that the majority of the remains from units UB4c and UB5a plotted at or very close to the contact between these two layers, the relatively high percentage of lithics in both units, as well as the absence of size sorting or grading, suggest autochthonous assemblages, deposited in UB5a and subsequently eroded *in situ* by the UA3/UB4 flood event.

5.3. Point pattern analysis

The hypothesis that in both areas the lithic and faunal assemblages were primarily deposited *in situ* and were subsequently somewhat reworked by a low energy flood, was further explored by means of point pattern analysis.

We assumed that a completely random spatial distribution of the lithic artefacts and faunal remains would suggest an allochthonous origin and subsequent transport to the site by the action of a random massive process, such as debris flow. Nevertheless, clustering of artefacts is not necessary evidence for human presence. Aggregation or segregation patterns could be produced by a range of biotic and/or natural processes. Human activities, topography and physical obstructions alike could trigger spatial aggregation.

The three-dimensional distribution of lithic artefacts from unit UA3c shows significant clustering for values of r between 35 and 65 cm. Lithic artefacts occur relatively close to the skeletal elements of the elephant, mostly about 20 cm apart and not more than 50 cm apart (Fig. 9). The richest cluster of about 20 lithic artefacts is located SW of the cranium, close to the right femur and the scatter of ribs and vertebrae.

Considering the prevalent NE orientation of the elephant bones and the other faunal remains from UA4, it is not unlikely that a SW/NE oriented flood could have been responsible for the observed accumulation SW of the elephant cranium, which would have represented an important obstruction to the flow. A similar case of clustering of small remains, apparently dammed by a long elephant tusk, has also been observed at Castel di Guido ([Boschian and Saccà, 2010](#)).

As mentioned above, whereas fairly random fabric and spatial distribution of coarse clasts are observed at the centre of modern debris flow deposits, preferential orientation and clustering may occur at the margin of the flood ([Pierson, 2005](#)). Yet the fabric analysis of the UA3c sample shows a random distribution, which falls within the range of debris flow (Fig. 6), and the pair correlation function (Fig. 9b) suggests significant clustering of lithic artefacts at relatively small scale: a pattern less likely to be produced by a large scale massive process such as a debris flow. Moreover, clusters of lithic artefacts occur as well in areas with less density of elephant bones.

Small scale clustering; proximity to the elephant remains and the erosional surface;

absence of spatial size sorting and, on the contrary, the presence of a relatively high number of lithic debris/chips associated with some flakes and tools; close anatomical spatial association of the elephant skeletal elements, slightly displaced and preferentially oriented: these lines of evidences support the hypothesis of an autochthonous primary deposition, subject to localised minor reworking.

A similar pattern can be observed in Area B, where a first set of spatial statistics confirmed that the inhomogeneous density of remains from unit UB4c (Fig. 10a) is not completely explained by the covariate effect of the underlying complex topography created by the erosional event UA3/UB4 (Fig. 3b).

Thus, we explored the relative spatial interaction between the UB4c and the underlying UB5a samples. We assumed that complete spatial randomness of the two independent depositional processes would occur in case of an exogenous origin and transportation of the UB4c assemblage. The hypothesis of an autochthonous original deposition of the faunal and lithic assemblages on the UB5a unit, subsequently eroded *in situ* by a relatively high energy flood (UB4c), was tested by cross-pattern spatial correlation functions (Figs. 10d,e). Whereas the two samples are vertically adjacent to the erosional surface (Fig. 8), on the horizontal plane they are both more segregated than expected for a random distribution.

Moreover, for the UB4c sample, an unsorted particle size spatial distribution was confirmed (Fig. 11). The occurrence in the same place of small and large classes of remains suggests that post-depositional processes, such as water winnowing, have not severely affected the assemblage. Hyperconcentrated flows would have dumped material on the lake margin. In this way, particles would have been frozen and deposited *en masse*. Hence their non-sorted spatial distribution.

On the other hand, the extraordinary preservation and number of mint to sharp, unsorted lithic artefacts from the UB4c unit; their density, positively correlated to the topography, and significantly segregated from the underlying distribution of remains; the vertical proximity of both assemblages from UB4c and UB5a to the erosional surface; as well as the random orientation pattern of the former, suggest that significant displacement of materials due to the erosional event can be excluded.

The faunal and lithic assemblages from unit UB4c therefore most likely derived

from the local erosion of exposed mudflat areas (UB5a layer) and have been slightly redistributed by the same flood event that capped the elephant in Area A.

Further evidence that the recovered assemblage has not undergone substantial reworking and has retained its original characteristics would come from the refitting analysis, currently in progress. To date, 4 bone refits have been found in Area B: three from unit UB4c, respectively at 4.771, 0.048 and 0.012 m distance; and one between two mammal bone fragments from units UB4c and UB5a, at a very short distance (0.086 m). Interestingly, one of the elements of the most distant refit (a *Dama* sp. mandibular fragment) shows traces of carnivore gnawing (Konidaris et al., this volume).

In conclusion, multiple lines of evidence suggest that the erosional event UB4/UA3 represents a relatively low-energy process in the continuum between debris and hyper-concentrated flow, which would have locally reworked at a small scale the already exposed or slightly buried and spatially associated lithic and faunal assemblages.

Although the UB4/UA3 process represents a snapshot of a relatively short frame of time, inferences about the use of space by human groups, in terms of knapping episodes and butchering activities, are unreliable in light of the current information.

The spatial pattern observed at the site is indeed the result of the last in a palimpsest of spatial processes. Whereas the erosional event represented by the debris/hyperconcentrated flow UA3/UB4 caps the sequence and preserves the record, little is known about the eroded underlying occupational horizon.

However, whereas hunting or scavenging is still an unsolved matter of debate, considering the bone fragmentation rate, the density of lithic debris/chips, the number of processed bones and their spatial density and association, it is likely that the assemblage represents a complex palimpsest of locally repeated events of hunting/scavenging and exploitation of lake shore resources.

More data from high resolution excavations in the coming years would allow us to refine the coarse-grained spatio-temporal resolution of our inferences about past human behaviour at Marathousa 1.

6. Conclusions

At the Middle Pleistocene open-air site of Marathousa 1 a partial skeleton of a single individual of *Elephas (Palaeoloxodon) antiquus* was recovered in stratigraphic association with a rich and consistent lithic assemblage and other vertebrate remains. Cut-marks and percussion marks have been identified on the elephant and other mammal bones excavated at the site. The main find-bearing horizon represents a secondary depositional process in a lake margin context.

Understanding the site formation processes is of primary importance in order to reliably infer hominin exploitation of the elephant carcass and other animals. To meet this aim, we applied a comprehensive set of multivariate and multiscale spatial analyses in a taphonomic framework.

Results from the fabric, vertical distribution and point pattern analyses are consistent with a relatively low-energy erosional process slightly reworking at a small scale an exposed (or slightly buried) and consistent scatter of lithic artefacts and faunal remains. These results are in agreement with preliminary taphonomic observations of the lithic artefacts (Tourloukis et al., this volume) and the faunal remains (Konidaris et al., this volume), which also indicate minor weathering and transportation. Our analyses show that multiple lines of evidence support an autochthonous origin of the lithic and faunal assemblages, subject to minor post-depositional reworking. Human activities therefore took place on-site, during an as of yet uncertain range of time.

Acknowledgements

This research is supported by the European Research Council (ERC StG PaGE 283503) awarded to K. Harvati. We are grateful to the Municipality of Megalopolis, the authorities of the Region of Peloponnese, and the Greek Public Power corporation (Δ EH) for their support. We also thank Julian Bega and all the participants in the PaGE survey and excavation campaigns in Megalopolis for their indispensable cooperation.

References

- Anderson, K. L., Burke, A., 2008. Refining the definition of cultural levels at Karabi Tamchin: a quantitative approach to vertical intra-site spatial analysis. *Journal of Archaeological Science* 35 (8), 2274–2285.
- Baddeley, A., Chang, Y.-M., Song, Y., Turner, R., 2012. Nonparametric estimation of the dependence of a point process on spatial covariates. *Statistics and Its Interface* 5 (2), 221–236.
- Baddeley, A., Rubak, E., Turner, R., 2015. *Spatial Point Patterns: Methodology and Applications* with R. Chapman and Hall/CRC, London.
- Bar-Yosef, O., Tchernov, E., 1972. On the palaeo-ecological history of the site of Ubeidiya. Vol. 35. Israel Academy of Sciences and Humanities, Jerusalem.
- Benito-Calvo, A., de la Torre, I., 2011. Analysis of orientation patterns in Olduvai Bed I assemblages using GIS techniques: Implications for site formation processes. *Journal of Human Evolution* 61 (1), 50 – 60.
- Benito-Calvo, A., Martínez-Moreno, J., Mora, R., Roy, M., Roda, X., 2011. Trampling experiments at Cova Gran de Santa Linya, Pre-Pyrenees, Spain: their relevance for archaeological fabrics of the Upper–Middle Paleolithic assemblages. *Journal of Archaeological Science* 38 (12), 3652–3661.
- Benito-Calvo, A., Martínez-Moreno, J., Pardo, J. F. J., de la Torre, I., Torcal, R. M., 2009. Sedimentological and archaeological fabrics in Palaeolithic levels of the South-Eastern Pyrenees: Cova Gran and Roca dels Bous Sites (Lleida, Spain). *Journal of Archaeological Science* 36 (11), 2566 – 2577.
- Benn, D., 1994. Fabric shape and the interpretation of sedimentary fabric data. *Journal of Sedimentary Research* 64 (4a), 910–915.
- Berman, M., 1986. Testing for spatial association between a point process and another stochastic process. *Applied Statistics* 35, 54–62.

- Bernatchez, J. A., 2010. Taphonomic implications of orientation of plotted finds from Pinnacle Point 13B (Mossel Bay, Western Cape Province, South Africa). *Journal of Human Evolution* 59 (3–4), 274 – 288.
- Bertran, P., Hetù, B., Texier, J.-P., Steijn, H. V., 1997. Fabric characteristics of subaerial slope deposits. *Sedimentology* 44 (1), 1 – 16.
- Bertran, P., Lenoble, A., Todisco, D., Desrosiers, P. M., Sørensen, M., 2012. Particle size distribution of lithic assemblages and taphonomy of Palaeolithic sites. *Journal of Archaeological Science* 39 (10), 3148 – 3166.
- Bertran, P., Texier, J.-P., 1995. Fabric Analysis: Application to Paleolithic Sites. *Journal of Archaeological Science* 22 (4), 521 – 535.
- Boschian, G., Saccà, D., 2010. Ambiguities in human and elephant interactions? Stories of bones, sand and water from Castel di Guido (Italy). *Quaternary International* 214 (1–2), 3 – 16.
- Carrer, F., 2015. Interpreting Intra-site Spatial Patterns in Seasonal Contexts: an Ethnoarchaeological Case Study from the Western Alps. *Journal of Archaeological Method and Theory*, 1–25.
- Clark, A. E., 2016. Time and space in the middle paleolithic: Spatial structure and occupation dynamics of seven open-air sites. *Evolutionary Anthropology: Issues, News, and Reviews* 25 (3), 153–163.
- Cobo-Sánchez, L., Aramendi, J., Domínguez-Rodrigo, M., 2014. Orientation patterns of wildebeest bones on the lake Masek floodplain (Serengeti, Tanzania) and their relevance to interpret anisotropy in the Olduvai lacustrine floodplain. *Quaternary International* 322–323 (0), 277 – 284.
- Diggle, P., 1985. A kernel method for smoothing point process data. *Applied Statistics (Journal of the Royal Statistical Society, Series C)* 34, 138–147.
- Domínguez-Rodrigo, M., Bunn, H., Mabulla, A., Baquedano, E., Uribelarrea, D., Pérez-González, A., Gidna, A., Yravedra, J., Diez-Martin, F., Egeland, C., Barba,

R., Arriaza, M., Organista, E., Ansón, M., 2014a. On meat eating and human evolution: A taphonomic analysis of BK4b (Upper Bed II, Olduvai Gorge, Tanzania), and its bearing on hominin megafaunal consumption. *Quaternary International* 322–323, 129–152.

Domínguez-Rodrigo, M., Bunn, H., Pickering, T., Mabulla, A., Musiba, C., Baquedano, E., Ashley, G., Diez-Martin, F., Santonja, M., Uribelarrea, D., Barba, R., Yravedra, J., Barboni, D., Arriaza, C., Gidna, A., 2012. Autochthony and orientation patterns in Olduvai Bed I: a re-examination of the status of post-depositional biasing of archaeological assemblages from FLK North (FLKN). *Journal of Archaeological Science* 39 (7), 2116 – 2127.

Domínguez-Rodrigo, M., Cobo-Sánchez, L., Yravedra, J., Uribelarrea, D., Arriaza, C., Organista, E., Baquedano, E., 2017. Fluvial spatial taphonomy: a new method for the study of post-depositional processes. *Archaeological and Anthropological Sciences*, 1–21.

Domínguez-Rodrigo, M., Diez-Martín, F., Yravedra, J., Barba, R., Mabulla, A., Baquedano, E., Uribelarrea, D., Sánchez, P., Eren, M. I., 2014b. Study of the SHK Main Site faunal assemblage, Olduvai Gorge, Tanzania: Implications for Bed II taphonomy, paleoecology, and hominin utilization of megafauna. *Quaternary International* 322–323, 153–166.

Domínguez-Rodrigo, M., García-Pérez, A., 07 2013. Testing the Accuracy of Different A-Axis Types for Measuring the Orientation of Bones in the Archaeological and Paleontological Record. *PLoS ONE* 8 (7), e68955.

Domínguez-Rodrigo, M., Uribelarrea, D., Santonja, M., Bunn, H., García-Pérez, A., Pérez-González, A., Panera, J., Rubio-Jara, S., Mabulla, A., Baquedano, E., Yravedra, J., Diez-Martín, F., 2014c. Autochthonous anisotropy of archaeological materials by the action of water: experimental and archaeological reassessment of the orientation patterns at the Olduvai sites . *Journal of Archaeological Science* 41 (0), 44 – 68.

- Eren, M. I., Durant, A., Neudorf, C., Haslam, M., Shipton, C., Bora, J., Korisettar, R., Petraglia, M., 2010. Experimental examination of animal trampling effects on artifact movement in dry and water saturated substrates: a test case from South India. *Journal of Archaeological Science* 37 (12), 3010 – 3021.
- García-Moreno, A., Smith, G. M., Kindler, L., Pop, E., Roebroeks, W., Gaudzinski-Windheuser, S., Klinkenberg, V., 2016. Evaluating the incidence of hydrological processes during site formation through orientation analysis. A case study of the middle Palaeolithic Lakeland site of Neumark-Nord 2 (Germany). *Journal of Archaeological Science: Reports* 6, 82 – 93.
- Gifford-Gonzalez, D., Damrosch, D., Damrosch, D., Pryor, J., Thunen, R., 1985. The Third Dimension in Site Structure: An Experiment in Trampling and Vertical Dispersal. *American Antiquity* 50 (4), 803–818.
- Giusti, D., Arzarello, M., 2016. The need for a taphonomic perspective in spatial analysis: Formation processes at the Early Pleistocene site of Pirro Nord (P13), Apricena, Italy. *Journal of Archaeological Science: Reports* 8, 235 – 249.
- Harvati, K., Panagopoulou, E., Tourloukis, V., Thompson, N., Karkanas, P., Athanasiou, A., Konidaris, G., Tsartsidou, G., Giusti, D., 2016. New Middle Pleistocene elephant butchering site from Greece. In: Paleoanthropology Society Meeting. Atlanta, Georgia, pp. A14–A15.
- Hivernel, F., Hodder, I., 1984. Analysis of artifact distribution at Ngenyem (Kenya): depositional and postdepositional effects. In: Hietala, H., Larson, P. (Eds.), *Intrasite Spatial Analysis in Archaeology*. Cambridge University Press, Ch. 7, pp. 97–115.
- Hodder, I., Orton, C., 1976. *Spatial Analysis in Archaeology*. New Studies in Archaeology. Cambridge University Press, Cambridge.
- Isaac, G. L., 1967. Towards the interpretation of occupation debris: Some experiments and observations. *Kroeber Anthropological Society Papers* 37 (37), 31–57.
- Jammalamadaka, S., Sengupta, A., Sengupta, A., 2001. *Topics in Circular Statistics. Series on multivariate analysis*. World Scientific.

- Lenoble, A., 2005. Ruissellement et formation des sites préhistoriques. Référentiel actualiste et exemple d'application au fossile. Vol. 1363 of International Series. British Archaeological Report, Oxford.
- Lenoble, A., Bertran, P., 2004. Fabric of Palaeolithic levels: methods and implications for site formation processes. *Journal of Archaeological Science* 31 (4), 457 – 469.
- Lenoble, A., Bertran, P., Lacrampe, F., 2008. Solifluction-induced modifications of archaeological levels: simulation based on experimental data from a modern periglacial slope and application to French Palaeolithic sites. *Journal of Archaeological Science* 35 (1), 99 – 110.
- López-Ortega, E., Bargalló, A., de Lombera-Hermida, A., Mosquera, M., Ollé, A., Rodríguez-Álvarez, X. P., 2015. Quartz and quartzite refits at Gran Dolina (Sierra de Atapuerca, Burgos): Connecting lithic artefacts in the Middle Pleistocene unit of TD10.1. *Quaternary International*, –.
- López-Ortega, E., Rodríguez, X. P., Vaquero, M., 2011. Lithic refitting and movement connections: the NW area of level TD10-1 at the Gran Dolina site (Sierra de Atapuerca, Burgos, Spain). *Journal of Archaeological Science* 38 (11), 3112 – 3121.
- Marwick, B., 2017. Computational reproducibility in archaeological research: Basic principles and a case study of their implementation. *Journal of Archaeological Method and Theory* 24 (2), 424–450.
- McPherron, S. J., 2005. Artifact orientations and site formation processes from total station proveniences. *Journal of Archaeological Science* 32 (7), 1003 – 1014.
- Morin, E., Tsanova, T., Sirakov, N., Rendu, W., Mallye, J.-B., Lèveque, F., 2005. Bone refits in stratified deposits: testing the chronological grain at Saint-Cesaire. *Journal of Archaeological Science* 32, 1083–1098.
- Morton, A. G. T., 2004. Archaeological Site Formation: Understanding Lake Margin Contexts. No. 1211 in BAR International Series. Archaeopress, Oxford.

- Nickel, B., Riegel, W., Schonherr, T., Velitzelos, E., 1996. Environments of coal formation in the Pleistocene lignite at Megalopolis, Peloponnesus (Greece) - reconstruction from palynological and petrological investigations. *N. Jb. Geol. Palaont. A.* 200, 201–220.
- Nielsen, A. E., 1991. Trampling the archaeological record: an experimental study. *American Antiquity* 56 (3), 483–503.
- Ohser, J., 1983. On estimators for the reduced second moment measure of point processes. *Mathematische Operationsforschung und Statistik, series Statistics* 14, 63–71.
- Organista, E., Domínguez-Rodrigo, M., Yravedra, J., Uribe Larrea, D., Arriaza, M. C., Ortega, M. C., Mabulla, A., Gidna, A., Baquedano, E., 2017. Biotic and abiotic processes affecting the formation of BK Level 4c (Bed II, Olduvai Gorge) and their bearing on hominin behavior at the site. *Palaeogeography, Palaeoclimatology, Palaeoecology*, –.
- Orton, C., 1982. Stochastic process and archaeological mechanism in spatial analysis. *Journal of Archaeological Science* 9 (1), 1 – 23.
- Panagopoulou, E., Tourloukis, V., Thompson, N., Athanassiou, A., Tsartsidou, G., Konidaris, G., Giusti, D., Karkanas, P., Harvati, K., 2015. Marathousa 1: a new Middle Pleistocene archaeological site from Greece. *Antiquity Project Gallery* 89 (343).
- Petraglia, M. D., Nash, D. T., 1987. The impact of fluvial processes on experimental sites. In: Nash, D. T., Petraglia, M. D. (Eds.), *Natural formation processes and the archaeological record*. Vol. 352 of International Series. British Archaeological Reports, Oxford, pp. 108–130.
- Petraglia, M. D., Potts, R., 1994. Water Flow and the Formation of Early Pleistocene Artifact Sites in Olduvai Gorge, Tanzania . *Journal of Anthropological Archaeology* 13 (3), 228 – 254.
- Pierson, T. C., 2005. Distinguishing between debris flows and floods from field evidence in small watersheds. Usgs numbered series, U.S. Geological Survey.

- R Core Team, 2016. R: A Language and Environment for Statistical Computing. R Foundation for Statistical Computing, Vienna, Austria.
- Rick, J. W., 1976. Downslope movement and archaeological intrasite spatial analysis. *American Antiquity* 41 (2), 133–144.
- Ripley, B., 1977. Modelling spatial patterns. *Journal of the Royal Statistical Society, series B* 39, 172–212.
- Ripley, B., 1988. Statistical inference for spatial processes. Cambridge University Press.
- Ripley, B. D., 1976. The second-order analysis of stationary point processes. *Journal of Applied Probability* 13 (2), 255–266.
- Ripley, B. D., 1981. Spatial Statistics. John Wiley and Sons, New York.
- Schick, K. D., 1984. Processes of paleolithic site formation: an experimental study. Ph.D. thesis, University of California, Berkeley.
- Schick, K. D., 1986. Stone Age sites in the making: experiments in the formation and transformation of archaeological occurrences. Vol. 319 of International Series. British Archaeological Reports, Oxford.
- Schick, K. D., 1987. Modeling the formation of Early Stone Age artifact concentrations. *Journal of Human Evolution* 16, 789–807.
- Schiffer, M. B., 1972. Archaeological Context and Systemic Context. *American Antiquity* 37 (2), 156–165.
- Schiffer, M. B., 1983. Toward the identification of formation processes. *American Antiquity* 48 (4), 675–706.
- Schiffer, M. B., 1987. Formation processes of the archaeological record. University of New Mexico Press, Albuquerque.
- Shackley, M. L., 1978. The behaviour of artefacts as sedimentary particles in a fluvial environment. *Archaeometry* 20 (1), 55–61.

- Sisk, M. L., Shea, J. J., 2008. Intrasite spatial variation of the Omo Kibish Middle Stone Age assemblages: Artifact refitting and distribution patterns . *Journal of Human Evolution* 55 (3), 486 – 500.
- Sánchez-Romero, L., Benito-Calvo, A., Pérez-González, A., Santonja, M., 12 2016. Assessment of Accumulation Processes at the Middle Pleistocene Site of Ambrona (Soria, Spain). Density and Orientation Patterns in Spatial Datasets Derived from Excavations Conducted from the 1960s to the Present. *PLOS ONE* 11 (12), 1–27.
- Todd, L., Stanford, D., 1992. Application of conjoined bone data to site structural studies. In: Hofman, J., Enloe, J. (Eds.), *Piecing Together the Past: Applications of Refitting Studies in Archaeology*. Vol. 578 of International Series. BAR, Oxford, pp. 21–35.
- van Vugt, N., de Bruijn, H., van Kolfschoten, M., Langereis, C. G., 2000. Magneto- and cyclostratigraphy and mammal-fauna's of the Pleistocene lacustrine Megalopolis Basin, Peloponnesos, Greece. *Geologica Ultrajectina* 189, 69–92.
- Vaquero, M., Bargalló, A., Chacón, M. G., Romagnoli, F., Sañudo, P., 2015. Lithic recycling in a Middle Paleolithic expedient context: Evidence from the Abric Romaní (Capellades, Spain). *Quaternary International* 361, 212 – 228.
- Vaquero, M., Chacón, M. G., García-Antón, M. D., de Soler, B. G., Martínez, K., Cuartero, F., 2012. Time and space in the formation of lithic assemblages: The example of Abric Romaní Level J. *Quaternary International* 247 (0), 162 – 181.
- Villa, P., 1982. Conjoinable Pieces and Site Formation Processes. *American Antiquity* 47 (2), 276–290.
- Villa, P., 1990. Torralba and Aridos: elephant exploitation in Middle Pleistocene Spain. *Journal of Human Evolution* 19 (3), 299 – 309.
- Villa, P., Courtin, J., 1983. The interpretation of stratified sites: A view from underground. *Journal of Archaeological Science* 10 (3), 267–281.

Voorhies, M., 1966. Taphonomy and population dynamics of an early Pliocene vertebrate fauna, Knox County, Nebraska. Ph.D. thesis, University of Wyoming.

Wood, R. W., Johnson, D. L., 1978. A survey of disturbance processes in archaeological site formation. In: Schiffer, M. B. (Ed.), Advances in archaeological method and theory. Vol. 1. Academic Press, Ch. 9, pp. 315–381.

Woodcock, N., Naylor, M., 1983. Randomness testing in three-dimensional orientation data. *Journal of Structural Geology* 5 (5), 539 – 548.